NeuroImage 331 (2026) 121883

Contents lists available at ScienceDirect

NeuroImage

journal homepage: www.elsevier.com/locate/ynimg

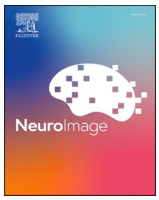

Generalizable prediction of hand motor behaviour from spontaneous brain connectivity

Enrica Pierotti [a], Luigi Cattaneo [a,b], Luca Turella [a,*]

[a] Center of Mind/Brain Sciences (CIMeC), University of Trento, Italy
[b] Centre for Medical Sciences (CISMED), University of Trento, Italy

ARTICLE INFO

Keywords:
Motor system
Hand
Action
TMS
fMRI
Functional connectivity
Resting state

ABSTRACT

Dexterous hand motor behavior emerges from coordinated interactions within a distributed brain network. While task-related neural dynamics have been investigated, recent fMRI studies showed that also spontaneous - i.e. non-task related - brain connectivity can predict task-specific performance. Still, it remains unclear whether spontaneous functional connectivity reflects also the encoding of general aspects of hand motor control.

Here, we applied connectome-based predictive modelling (CPM) to resting-state functional connectivity (rs-FC) from the Human Connectome Project (HCP) to predict performance in hand motor tasks. We identified a "core" hand motor network whose intrinsic connectivity predicted not only task-specific measures (dexterity and strength) but generalised its prediction across different effectors and tasks.

This "core" model also generalized its predictions to an independent dataset (external validation), including different behavioral measures and rs-fMRI data. In addition, transcranial magnetic stimulation (TMS) over inferior parietal cortex selectively impacted the core model's predictive power in a time-dependent manner, consistent with the known neurophysiological effects of the stimulation protocol.

Together, these findings demonstrate that spontaneous brain activity encodes behaviorally relevant information about hand motor control, spanning both low-level features and higher-order representations. By linking spontaneous brain activity to behavioural motor outcomes, our findings pave the way for better understanding how spontaneous connectivity alterations might underlie motor dysfunction in neurological disorders.

1. Introduction

Dexterous hand movements rely on the representation of action-related information within a widespread brain network. Traditionally, task-related functional connectivity has been used to study these networks. However, recent findings show that also spontaneous connectivity can predict behavioral performance. For instance, whole-brain resting-state functional connectivity (rs-FC) has been shown to predict specific movement feature, such as grip strength (e.g. Wu et al., 2021). However, it remains unclear whether rs-FC captures not only task-specific measures but also more general aspects of hand motor control - representations that are independent of the specific effector or task employed.

An extensive corpus of fMRI studies has shown the consistent recruitment of a wide network of cortical, subcortical and cerebellar regions during the performance of hand actions (Culham et al., 2006; Culham and Valyear, 2006; Errante et al., 2021; Gallivan and Culham, 2015; Grafton, 2010; Sartin et al., 2023; Turella and Lingnau, 2014; Vesia and Crawford, 2012). Multivariate decoding approaches have further revealed the fine-grained specialization of these regions, showing decoding of information about specific aspects of hand movements (Gallivan and Culham, 2015), such as effector (Gallivan et al., 2013) or action type (Gallivan et al., 2013, 2011; Malfatti and Turella, 2021; Monaco et al., 2020, 2019; Turella et al., 2020). Recent MVPA studies showed also that it is possible to define regions hosting more "abstract" information, such as decoding action representations across effectors (Gallivan et al., 2013; Turella et al., 2020) or tasks (Monaco et al., 2020). This view aligns with the classical hierarchical organization of the motor system, where behavior is represented at multiple levels of abstraction. Whether similar abstract information about hand actions is also embedded in spontaneous brain connectivity, however, remains unknown.

To address this question, we employed Connectome-based Predictive Modeling (CPM) which is a data-driven approach that links brain

* Corresponding author at: Center for Mind/Brain Sciences (CIMeC), University of Trento, Corso Bettini 31, Rovereto, TN, 38068, Italy.
E-mail address: luca.turella@unitn.it (L. Turella).

https://doi.org/10.1016/j.neuroimage.2026.121883
Received 8 October 2025; Received in revised form 10 March 2026; Accepted 24 March 2026
Available online 25 March 2026

connectivity with behavioral variables (Shen et al., 2017; Wu et al., 2023). This approach has been adopted to establish brain-behavior correlations across multiple cognitive domains. Previous studies have demonstrated that CPM can be employed to predict individual psychometric and behavioral variables from patterns of FC in both healthy participants (e.g., Rosenberg et al., 2016; Shen et al., 2017; Wu et al., 2022; Yoo et al., 2022) and clinical populations (Kim et al., 2023; Lake et al., 2019; Rabini et al., 2023). In healthy individuals, CPM has been employed to predict fluid intelligence (Finn et al., 2015; Wu et al., 2022; Yoo et al., 2019), attention (Rosenberg et al., 2018, 2016; Shen et al., 2017; Yoo et al., 2022, 2018), working memory (Avery et al., 2020; Zhang et al., 2020), creativity (Beaty et al., 2018) and personality traits (Cai et al., 2020; Hsu et al., 2018; Jiang et al., 2018). In clinical populations, CPM has been applied to predict clinical scores for depression (Kim et al., 2023), severity of motor symptoms in Parkinson's disease (Rabini et al., 2023) and social abilities in autism and attention deficit hyperactivity disorder (Lake et al., 2019). Crucially, CPM can also capture higher-order domain-general representations - for example, predicting attentional abilities across tasks, datasets and even months apart (Rosenberg et al., 2016, 2017, 2020 ; Yoo et al., 2022).

Building on this framework, we had three aims. First, using the Human Connectome Project (HCP) dataset, we sought to identify a brain network whose rs-FC could predict performance in two distinct tasks, measuring dexterity (Nine-Hole Peg Test) and strength (isometric grip force task), performed separately with the two hands. We anticipate that we could find a network of regions - a "core" hand motor network – whose connectivity predicted three (out of four) specific motor tasks of the HCP dataset (right-hand dexterity, right-hand strength and left-hand strength). Second, we tested whether this core network generalized beyond specific task demands, predicting individual behavioural performance across different effectors and motor tasks. Third, we evaluated the generalizability of this core model to an independent dataset (external validation), assessing its predictive validity for novel behavioral measures of a different motor task. Finally, we probed its specificity by applying transcranial magnetic stimulation (TMS) to perturb a parietal region known to be involved in hand action, testing whether this intervention altered CPM's predictive performance.

2. Materials and methods

2.1. HCP dataset: participants and behavioural tasks

We analyzed anatomical and rs-fMRI data from the HCP dataset (Van Essen et al., 2013, 2012). The scanning protocol was approved by the Institutional Review Board at Washington University in St. Louis. All subjects gave written informed consent in accordance with the Washington University Institutional Review Board.

Participants. Although the full HCP sample includes 1200 healthy young adults, we restricted our analysis to individuals with a consistent rightward hand preference, defined by an Edinburgh Handedness Inventory score (EHI, Oldfield, 1971) greater than zero. This inclusive criterion was chosen over a stricter threshold for strong right-handedness (EHI $>$ 40) to maximize sample size and preserve statistical power in line with a recent behavioural evaluation of handedness using the HCP dataset (Ruck and Schoenemann, 2021). This approach identified a total of 1026 participants.

From this subset, we selected 969 participants (535 females; age range: 22–36 years) who met the following criteria: 1) completion of at least one rs-fMRI run with left-right phase encoding; 2) completion of the two behavioral motor tasks relevant to this study.

Behavioral tasks. The HCP includes a comprehensive battery of cognitive and motor assessments (Hodes et al., 2013). For the present study, we focused on two tasks measuring hand motor function. The first task was the Nine-Hole Peg Test (Mathiowetz et al., 1985) which assesses fine hand dexterity. Participants were instructed to insert and - then remove - nine pegs from a pegboard as quickly as possible with one hand at the time. As behavioral measure, we considered the time to complete the task (in seconds), recorded separately for the right and left hands.

The second task was the Grip Strength test (Hodes et al., 2013) which assesses upper limb strength. Participants used a hand-held dynamometer to exert maximal grip force, one hand at a time. The considered behavioral measure was the maximum exerted force (in pounds) measured separately for the right and left hands.

2.2. HCP dataset: MRI data acquisition and preprocessing

MRI data acquisition. Each participant completed two runs of rs-fMRI with opposite phase encoding directions: left-to-right (LR) and right-to-left (RL). For the present analysis, we used only the LR run. Each run consisted of 1200 vol acquired in 14.33 min (TR = 720 ms, TE = 33.1 ms, 72 slices, 2 mm isotropic voxels, Van Essen et al., 2012; Smith et al., 2013).

Preprocessing. We used the "minimally preprocessed" data provided by the HCP, which included motion correction and spatial normalization to MNI152 standard space (Glasser et al., 2013). Additional denoising was performed using ICA-FIX, which applies independent component analysis (ICA) to decompose the signal and a trained classifier (FIX) to automatically remove artifactual components (Griffanti et al., 2014; Salimi-Khorshidi et al., 2014; Smith et al., 2013).

2.3. Dataset for external validation: participants, kinematic and offline TMS-fMRI sessions

To validate the generalizability of our CPM, we employed an independent dataset comprising kinematic recordings and rs-fMRI data acquired before and after TMS. Part of this dataset have been previously published elsewhere (Pierotti et al., 2025).

Participants. Thirty-two right-handed participants participated in the study. Participants were excluded if they exhibited excessive head motion during fMRI acquisition (maximum displacement $>$ 2 mm; $n = 5$) or experienced technical issues during kinematic data acquisition ($n = 1$). The final sample comprised 26 right-handed participants (16 females, average age: 24 years). Participants had no contraindications to MRI or TMS investigation. They provided written informed consent to participate in the study and were reimbursed for their participation. The protocol of this study was approved by the Ethics Committee of Human Research of the University of Trento (protocol 2018–015).

Kinematic session. On a separate day from the neuroimaging session, participants completed a motor task involving grasping and reaching actions toward a small spherical object (4 cm diameter, placed 30 cm from the starting point; see Budisavljevic et al., 2017 for a similar design). In the grasping condition, participants used a precision grip (thumb and index finger) to grasp the object. In the reaching condition, they reached and touched the object with their knuckles. Each action was executed 15 times with each hand in separate blocks (one block per hand with block order counterbalanced across participants). In each block, an auditory cue indicated both the type of action (grasp or reach) and the go signal for movement initiation. Subjects were instructed to start the movement as fast as possible in response to this go signal. This design allowed us to record not only movement kinematics but also the reaction times associated with each action.

Kinematics data were recorded using a Qualysis Track Manager System (Qualisys AB, https://www.qualisys.com/) including five infrared cameras (ProReflex MCU) sampling at 100 Hz. Five markers were applied to participants' hands: on the thumb distal phalange, on the index finger distal phalange, on the metacarpophalangeal joint of the middle finger, and two on the wrist (distal radius and ulna).

From this task, we extracted three behavioral measures per hand: 1) reaction time (RT) during grasping, 2) RT during reaching, 3) maximum grip aperture (MGA) during grasping, defined as the maximum distance between the thumb and index markers throughout the movement.

Offline TMS-fMRI session. Each participant underwent two rs-fMRI runs before and two rs-fMRI runs after offline continuous theta-burst stimulation (cTBS; Huang et al., 2005) applied to the left human anterior intraparietal area (hAIP) - a key region involved in hand motor control (Grefkes and Fink, 2005). We selected the hAIP as our stimulation target based on extensive evidence that TMS applied over this region impacts different aspects of goal-directed hand actions (Breveglieri et al., 2023; Glover et al., 2005; Gutteling et al., 2013; Rice et al., 2007, 2006; Tunik et al., 2008, 2005). We adopted a neuronavigation system (SofTaxic system, software version 3.4, EMS, Italy) to localize hAIP on the reconstruction of individual brain images adopting anatomical landmarks. At the group level, the site of stimulation was located at the following mean MNI coordinates: x= -52 ± 6, y= -43 ± 5, z = 57 ± 4.

On the same day, each participant carried out the offline TMS-fMRI experimental session following a fixed order of stimulation. The experimental session comprised two resting states fMRI runs collected after sham cTBS and two resting states fMRI runs collected after real cTBS. The session started with the delivery of sham cTBS stimulation on hAIP outside the MR scanner room. After the sham stimulation, the participant was positioned in the MR scanner and underwent two runs of rs-fMRI before real TMS. Then, the participant was moved outside the MR scanner and real cTBS was delivered on the hAIP. Following stimulation, the subject was repositioned inside the MR scanner and underwent two runs of rs-fMRI after real TMS. Each rs-fMRI run lasted 10 min. For more information on the TMS-fMRI session, please refer to the previous publication (Pierotti et al., 2025).

2.4. Dataset for external validation: MRI data acquisition and preprocessing

MRI data acquisition. The rs-fMRI data were collected using a 3T Siemens MAGNETOM Prisma scanner (Siemens Healthcare, Erlangen, Germany) equipped with a 64-channel head coil. Each rs-fMRI run lasted 10 min and consisted of 600 vol (TR = 1 s, TE = 28 ms, 66 slices, voxel size = 3 mm isotropic). To correct geometric distortions, double-echo gradient echo field maps were acquired (TR = 4810 ms; TEs = 4.92 and 7.38 ms; voxel size = 3 mm isotropic Additionally, a high-resolution T1-weighted structural image was obtained using a multi-echo MPRAGE sequence (TR = 2500 ms; TEs = 1.69, 3.55, 5.41, 7.27 ms; voxel size = 1 mm isotropic).

Preprocessing. MRI data was preprocessed using SPM12 (https://www.fil.ion.ucl.ac.uk/spm/software/spm12/) with the following preprocessing steps: 1) slice-timing correction; 2) head motion correction; 3) distortion correction using the gradient echo-sequences; 3) T1-weighted segmentation to obtain the deformation field for the MNI normalization; 4) normalization to the MNI space; 5) Bandpass filtering (0.1–0.01 Hz). Finally, we resampled voxel size to match the whole brain parcellation (2 mm isotropic voxels).

3. CPM models

3.1. Parcellation atlas and functional connectivity estimation

Parcellation atlas. To estimate whole-brain functional connectivity, we employed a parcellation approach that combined cortical, subcortical and cerebellar regions, resulting in comprehensive anatomical coverage (Fig. 1). This composite atlas included 348 parcels distributed across nine functional networks.

Cortical regions were defined using the 300-parcel version of the Schaefer atlas (Schaefer et al., 2018), which is organized according to the seven canonical resting-state networks proposed by Yeo et al. (2011): 1) FrontoParietal, 2) Default Mode, 3) Dorsal Attention, 4) Limbic, 5) Ventral Attention, 6) Somatomotor, 7) Visual.

Subcortical regions were derived from an atlas based on previous work (Glasser et al., 2016; Gordon et al., 2016) comprising 16 parcels (bilateral: Hippocampus, Amygdala, Posterior and Anterior Thalamus, Nucleus Accumbens, Globus Pallidus, Putamen, and Caudate Nucleus) grouped into a single Subcortical network.

Cerebellar regions were extracted from a recent cerebellar atlas (Nettekoven et al., 2023), including 32 parcels that formed the Cerebellar network.

Functional connectivity estimation. Using this customized parcellation,

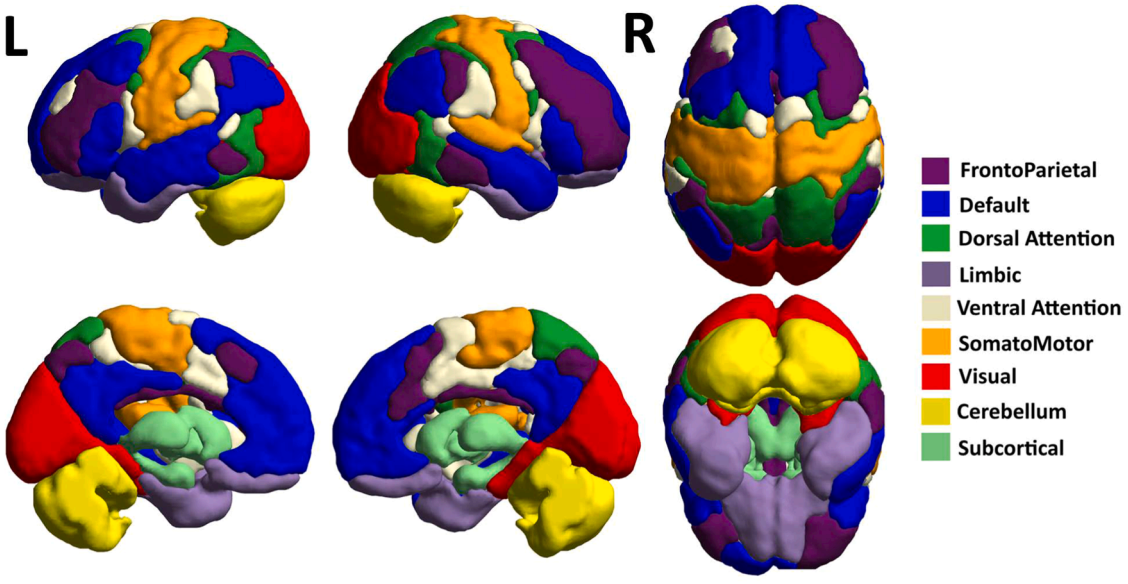

Fig. 1. Customized whole-brain parcellation and functional network organization. The figure illustrates the parcellation scheme adopted in the present study, comprising 348 regions across nine functional networks. This composite atlas was created by integrating: 1) a cortical parcellation (Schaefer et al., 2018; Thomas Yeo et al., 2011); 2) a cerebellar parcellation (Glasser et al., 2016; Gordon et al., 2016), and a subcortical parcellation (Nettekoven et al., 2023). From left to right, the top row displays lateral views of the left and right hemispheres, and a coronal view. The bottom row presents medial views of the left and right hemispheres, along with an axial (bottom-up) view. The nine functional networks are color-coded as follows: fronto-parietal network (dark purple); default mode network (blue); dorsal attention network (dark green); limbic network (light purple); the ventral attention network (cream); somato-motor network (orange); visual network (red); the cerebellum(yellow); the subcortical network (light green).

we extracted FC from both the HCP dataset and the external validation rs-fMRI dataset. The analysis was performed using custom MATLAB scripts (Version R2017b, The MathWorks Inc., https://www.mathworks.com). For each participant, we computed pairwise Pearson correlation coefficients between the mean time series of each parcel and every other parcel in the atlas. This procedure resulted in an individual 348 × 348 whole-brain FC matrix. All FC estimates were transformed using Fisher's z-transformation.

3.2. Whole brain CPM for predicting hand motor behaviour (HCP dataset)

Whole-brain CPMs. We started by testing if the CPM framework could be adopted to predict behavioral variables from whole brain FC, i.e. to try to establish a link between rs-FC and hand motor functioning. To this aim, we applied Support Vector Regression (SVR) to the rs-FC matrices obtained from our 348-region parcellation, modelling each motor variable separately. Specifically, we constructed independent CPM models to predict the following four behavioral measures: 1) left-hand dexterity (Nine-Hole Peg test); 2) right-hand dexterity (Nine-Hole Peg test); 3) left-hand strength (Grip Strength test); and 4) right-hand strength (Grip Strength test). All behavioral scores were z-scored prior to modeling.

We employed 10-fold cross-validation to evaluate each model. In each iteration, data from nine folds served as the training set, while the remaining fold was used for testing. To minimize data leakage, family members were kept within the same fold. Then, we computed the Pearson correlation coefficient between the predicted and observed behavioral scores in the test set, which served as an index of model accuracy. This entire procedure was repeated 1000 times and the resulting correlation coefficients were z-scored and averaged across repetitions.

To determine statistical significance, we adopted a non-parametric permutation approach. Specifically, we permuted the behavioral scores within each iteration of the cross-validation (1000 repetitions), generating a null distribution of correlation values (1000 values). We then compared the observed average correlation with this null distribution. False Discovery Rate (FDR) correction (Benjamini and Hochberg, 1995) was applied to correct for multiple comparisons.

Weights for Whole-brain CPMs. For each model, we also extracted and analysed the model weights, representing the functional connections (i.e. model features) contributing most to prediction. Direct interpretation of weights can be misleading, so we applied the Haufe transformation (Haufe et al., 2014), which converts the weights into interpretable values. After transformation, larger absolute values indicate greater relevance of specific connections in predicting the behavioral outcome (Haufe et al., 2014; Scheinost et al., 2019; Wu et al., 2023). We averaged these transformed weights across folds and repetitions to generate a final weight matrix for each behavioral model.

To assess the significance of individual connections, we again used a non-parametric approach. For each model, we generated null distributions by permuting behavioral values and recalculating the transformed weights (1000 permutations). Observed average weights were then compared to these null distributions, and FDR correction (Benjamini and Hochberg, 1995) was applied to control for multiple comparisons across the matrix.

3.3. Identification of a core hand motor network and test of its predictive power (HCP dataset)

Our first objective was to determine whether a core hand motor network could be identified across multiple behavioral tasks and whether this network alone could predict motor performance.

As described in the Results section ("Whole-brain CPM, identification of the core hand motor network and test of its predictive power"), three out of four whole-brain CPM models yielded significant predictions: dexterity of the right hand, strength of the left hand and strength of the right hand.

To define the core hand motor network, we first extracted all the significantly predictive connections (based on FDR-corrected Haufe-transformed weights) from each of these three models. Then, we calculated the intersection of these connections across the three models. While each whole-brain model included 60,552 unique pairwise connections (based on the 348 × 348 symmetric matrix), the core network consisted of 1833 connections.

We tested the predictive power of this core network by conducting the same CPM analyses using only these 1833 connections. We followed the same SVR and cross-validation procedure described in the previous section. This allowed us to evaluate whether the core network CPM could predict each of the four behavioral motor variables: dexterity for the left hand, dexterity for the right hand, strength for the left hand, strength for the right hand. Crucially, we also investigated whether these predictions were specific to the motor domain. To this aim, we tested the predictive power of the core CPM to non-motor HCP measures - fluid intelligence, personality and working memory - to verify that the network did not capture more general cognitive aspects (see *HCP dataset: Control Analyses on Non-Motor Variables* section in Supplementary Material).

3.4. Generalization of the core hand motor network CPM to different motor variables (HCP dataset)

The second aim of our study was to evaluate whether the core network captures more general aspects of hand motor control - beyond the specific motor variable used for training. In detail, we tested whether CPM model trained to predict a specific motor variable (e.g. force) could also predict the same variable for the opposite hand and/or a different motor variable (e.g. dexterity). This analysis allowed us to investigate whether the core network encodes higher-order aspects of motor control and not only task-specific motor variables.

As in our previous analyses, we employed a 10-fold cross-validation scheme with 1000 repetitions. To evaluate statistical significance, we generated null distributions by permuting behavioral values within each motor variable before computing the CPM (1000 permutations). False Discovery Rate (FDR) correction (Benjamini and Hochberg, 1995) was applied to correct for multiple comparisons.

3.5. External validation and network perturbation analysis of the core hand motor network CPM (HCP and external validation datasets)

Our final objective was to evaluate the generalizability of the core hand motor network CPM by testing its predictive performance on an independent dataset that included both new rs-fMRI data and different behavioral measures (external validation).

One of the primary challenges in the CPM framework is overfitting, where a model captures noise specific to the training dataset rather than true signal. This risk can be mitigated through external validation, which evaluates model performance on a separate dataset independent from the one adopted in the training phase. Such a procedure enhances the robustness and reproducibility of the findings by ensuring that the test data cannot influence model optimization (Scheinost et al., 2019).

We leveraged the unique structure of our external validation dataset, in which each participant contributed four rs-fMRI runs and six behavioral kinematic measures: RTs (separately for reaching and grasping actions) and maximum grip aperture (MGA) for both hands.

This allowed us to evaluate model performance in two distinct external validations: 1) unperturbed external validation using the two rs-fMRI runs acquired before real cTBS (but after sham stimulation); 2) perturbed external validation using the two rs-fMRI runs acquired after real cTBS over the left hAIP, a key region involved in hand motor control.

For the unperturbed external validation, we applied the core CPM model trained on the HCP dataset ($N = 969$) separately to the two pre-

TMS runs from the external sample ($N = 26$), assessing whether the model could predict new motor behavior based on FC in a different population. Specifically, we tested the three CPM models that showed significant performance in the training dataset (left-hand dexterity, left-hand strength, right-hand strength), using them to predict RT and MGA values in the independent sample.

For the perturbed external validation, we repeated the analysis using the two post-TMS runs. This allowed us to examine whether offline cTBS to the left hAIP would alter the predictive performance of the core CPM.

In both analyses, we computed Pearson correlation coefficients between the predicted and actual behavioral values to quantify model performance. To assess statistical significance, we generated a null distribution for each model by permuting the behavioral labels (1000 times) and compared the observed correlation coefficients to these null distributions. Statistical significance was determined by comparing the true correlation value against its corresponding null distribution. False Discovery Rate (FDR) correction (Benjamini and Hochberg, 1995) was applied to correct for multiple comparisons.

4. Results

4.1. Prediction of hand motor variables from whole-brain functional connectivity (HCP dataset)

We started by testing whether whole-brain rs-FC could predict performance in different motor tasks. Using CPM trained on the HCP dataset, we tested four separate models targeting different motor variables. Three of the four CPMs significantly predicted behavior: right-hand dexterity and strength for both hands ($p < 0.005$ FDR-corrected; see Fig. 2).

In the whole-brain analyses, we adopted a conservative approach ($p < 0.005$ FDR-corrected), as the objective was to constrain as much as possible the number of possible connections included within the core hand motor network (see next section).

4.2. Prediction of hand motor variables from the core hand motor network functional connectivity (HCP dataset)

Our first objective was to identify a core network, i.e. a subset of functional connections that consistently predicted performance in different hand motor tasks. To this end, we extracted the statistically significant connections from the three whole-brain CPMs that showed predictive power (right-hand dexterity, left-hand strength and right-hand strength) and computed their intersection. This procedure yielded a core network composed of 1833 connections.

Fig. 3A illustrates the distribution of these connections across the nine functional networks defined by our customized parcellation. Notably, the most frequent connections were between the Somatomotor and Default Mode networks, Default Mode and Fronto-Parietal networks, Somatomotor and Fronto-Parietal networks, Somatomotor and Visual networks, and between the Dorsal and Ventral Attention networks. Within-network connections were most prominently represented within the Default Mode Network.

As previously described (see Methods), we used a customized whole-brain parcellation combining cortical (Schaefer et al., 2018; Yeo et al., 2011), subcortical (Glasser et al., 2016; Gordon et al., 2016), and cerebellar (Nettekoven et al., 2023) atlases. The cortical large-scale networks were defined based on rs fMRI data, preserving their original naming conventions (Yeo et al., 2011) to facilitate comparison with previous studies. Still, it is important to note that there is not a consensus on the nomenclature and function of this networks (Biswal and Uddin, 2025). For this reason, Fig. 3B shows the spatial distribution of parcels involved in the core network. The color code depicts the number of significant connections for each parcel.

We then tested whether the core network CPM alone could predict hand motor variables, applying the same procedure adopted with whole brain data, but limiting the features to the 1833 core connections. As shown in Fig. 3C, the core CPM successfully predicted the same three behavioral measures as the original whole-brain models: right-hand dexterity and left/right-hand strength ($p < 0.005$ FDR-corrected). Moreover, we tested whether the core CPM was specific to predict hand motor variables or could also predict other non-motor behavioural measures of the HCP (fluid intelligence, personality and working memory). None of these models reached statistical significance ($p > 0.16$ uncorrected, see *Results of Control Analyses on Non-Motor Variables* section and Figure S1 in Supplementary Material).

These results indicate that the identified core network - despite being much smaller than the whole-brain connectivity matrix (1833 vs. 60,552 connections) - is functionally associated with upper-limb motor performance.

4.3. Generalization of the predictive performance of the core hand motor network CPM to different motor variables (HCP dataset)

Our second aim was to evaluate whether the core CPM captures general features of hand motor functioning, beyond adopted effectors or

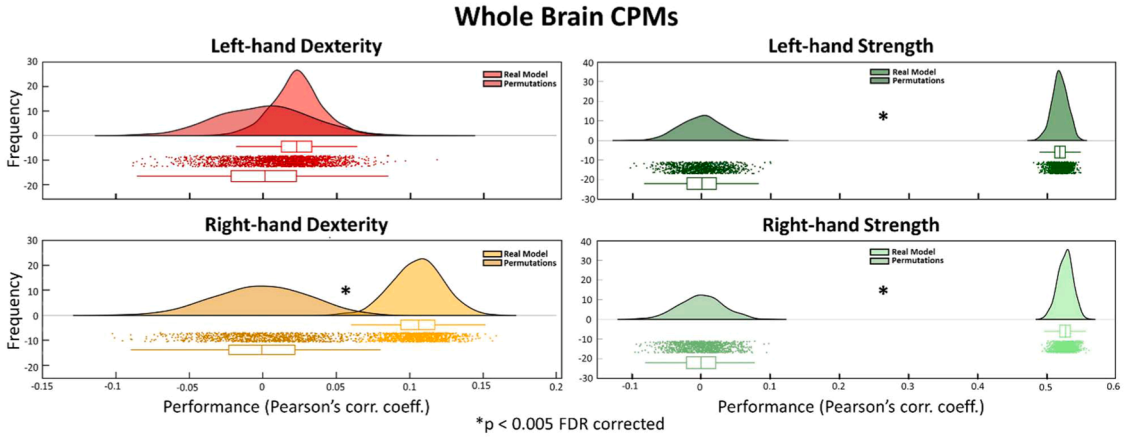

Fig. 2. Prediction performance of whole-brain CPMs for hand motor variables (HCP dataset). Each panel displays the distribution of model performance (Pearson's correlation between predicted and actual behavioral scores) for the real CPM compared to the null distribution obtained via permutation testing. The top-left panel shows the non-significant model for left-hand dexterity. The bottom-left panel shows a significant model for right-hand dexterity. The top-right and bottom-right panels show significant models for left-hand and right-hand strength, respectively. All significant results passed false discovery rate correction ($p < 0.005$ FDR-corrected).

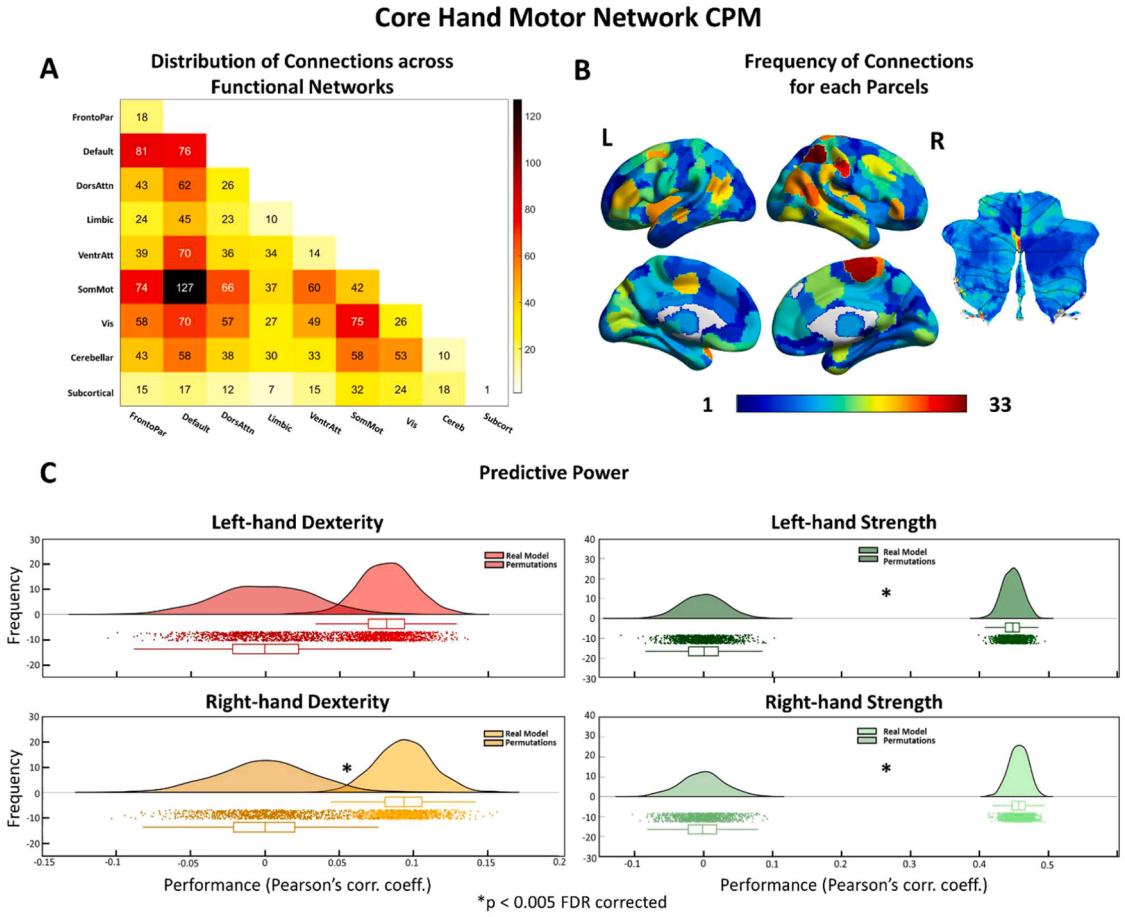

Fig. 3. Core hand motor network and its predictive performance. A. Distribution of connections across functional networks. The heatmap shows the number of connections within and between functional networks that comprise the core hand motor network (1833 connections). FrontoPar = fronto-parietal network; Default = default mode network; DorsAtt = dorsal attentional network; Limbic = limbic network; VentrAtt = ventral attentional network; SomMot = somatomotor network; Vis = visual network; Cerebellar = cerebellum; Subcortical = subcortical network. B. Spatial distribution of parcels in the core network. Brain surface maps show the frequency with which each parcel was involved in the core network. Frequencies reflect how often a parcel appeared across the significant connections shared by the three predictive whole-brain CPMs (right-hand dexterity, left-hand strength, and right-hand strength). C. Predictive power of the core network. Each panel displays the distribution of model performance (Pearson's correlation between predicted and actual behavioral scores) for the real CPM compared to the null distribution obtained via permutation testing. The model significantly predicted right-hand dexterity, left-hand strength, and right-hand strength ($p < 0.005$ FDR corrected, blue asterisks), but not left-hand dexterity.

specific task requirements. To address this, we employed a cross-generalization approach in which the CPM was trained on one motor variable and tested across tasks (dexterity vs. strength), across hands (right vs. left) or across both.

Several cross-generalization comparisons yielded significant results, indicating that core CPMs trained on a specific motor task can generalise their prediction to different motor tasks (see Fig. 4). First, core CPM trained on right-hand strength significantly predicted dexterity of the same hand and vice versa (see Fig. 4A). These results suggest that the core network captures task-independent information about motor performance, regardless of the specific requirement of the task (i.e., dexterity vs. strength).

Second, core CPM trained on strength for one hand (e.g., left) could significantly predict strength for the opposite hand (e.g., right) and vice versa (see Fig. 4B). This result indicates that this network encodes effector-independent information, generalizing across the left and right hands for the same type of motor task.

Finally, core CPM trained on right-hand dexterity significantly predicted left-hand strength and vice versa (Fig. 4C). These findings suggest that this network integrates broader action-related information that supports general motor performance across motor domains and effectors.

Taken together, these results highlight the generalizability of the core CPM across different motor domains, supporting the idea that it encodes higher-order neural representations of upper-limb motor control.

4.4. *Generalization of the predictive performance of core network CPM to an independent dataset (HCP and external validation datasets)*

To evaluate the generalizability of the core CPM beyond the original dataset, we tested its predictive performance on an independent sample comprising rs-fMRI and kinematic data. This external validation dataset included behavioral measures that differed from the ones of the HCP dataset: reaction times (RTs) for grasping and reaching tasks, and maximum grip aperture (MGA), a key kinematic parameter associated with skilled hand control. These measures were assessed for both hands separately. We reported the distributions of these behavioural measures in Supplementary Material (see *Dataset for external validation: Inter-individual variability of behavioural measures* section).

The inclusion of these novel motor variables allowed us to assess whether the core network CPM could generalize to different dimensions of motor behavior - ranging from a general index of action preparation (RTs) to more specific aspects associated with dexterous hand action

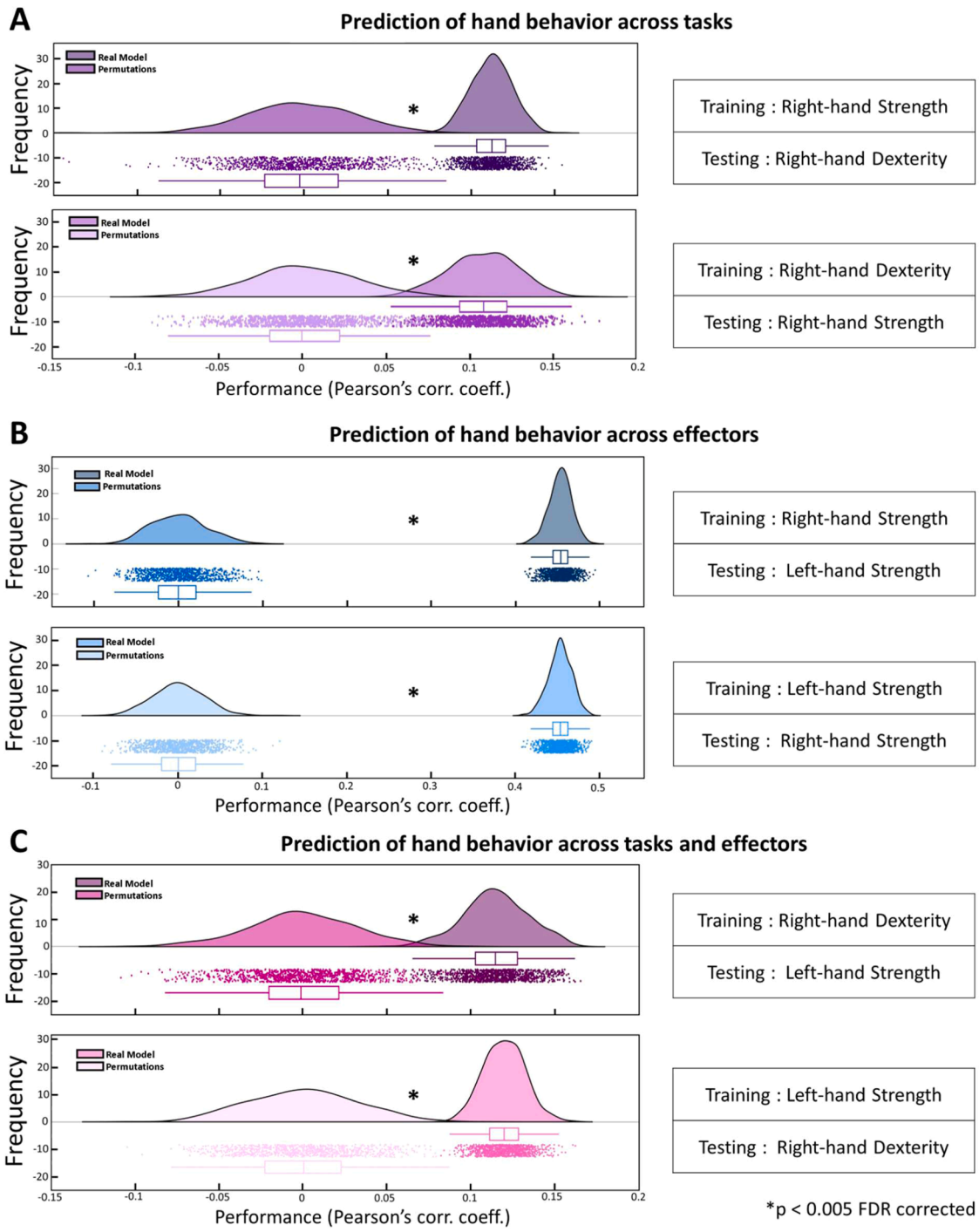

Fig. 4. Cross-generalization results of the core CPM. A. Task-independent cross-generalization. Distributions of model performance compared against the null distribution obtained through permutations. The y-axis displays Pearson's correlation coefficients (prediction accuracy) and the x-axis shows the cross-generalization comparison. B. Effector-independent cross-generalization. Distributions of model performance compared against the null distribution obtained through permutations. The y-axis displays Pearson's correlation coefficients (prediction accuracy), and the x-axis shows the cross-generalization comparison. C. Task- and effector-independent cross-generalization. Distributions of model performance compared against the null distribution obtained through permutations. The y-axis displays Pearson's correlation coefficients (prediction accuracy), and the x-axis shows the cross-generalization comparison. All models showed significant predictive power ($p < 0.005$ FDR corrected), supporting the hypothesis that the core network captures action-related information that extend beyond specific tasks or effectors.

execution (MGA).

Fig. 5 summarizes the external validation results across four rs-fMRI runs. The different panels (A–D) represents a separate run presented in temporal order. The columns in each panel depict the HCP-trained CPMs (based on different motor tasks and hands) and rows represent the target behavioral variables from the independent dataset. Prediction significance is indicated by red-colored correlation coefficient ($p < 0.05$ FDR corrected).

Fig. 5A displays the prediction results for the first rs-fMRI run acquired after sham TMS, but prior to real TMS which represents an "unperturbed" FC state. Significant predictions were observed for MGA of the right hand when the model was trained on right-hand dexterity in the HCP dataset. Similarly, MGA for the left hand was significantly predicted across three HCP training models (right-hand dexterity and

External Validation

Run 1 before TMS: unperturbed FC

		TRAINING DATASET		
		RIGHT-HAND DEXTERITY	RIGHT-HAND STRENGHT	LEFT-HAND STRENGHT
RIGHT HAND	RT REACHING	0.08	-0.19	-0.12
	RT GRASPING	0.21	-0.15	-0.06
	MGA	**0.45**	0.19	0.22
LEFT HAND	RT REACHING	-0.02	0.05	-0.12
	RT GRASPING	-0.02	0.07	-0.10
	MGA	**0.43**	**0.45**	**0.37**

Run 2 before TMS: unperturbed FC

		TRAINING DATASET		
		RIGHT-HAND DEXTERITY	RIGHT-HAND STRENGHT	LEFT-HAND STRENGHT
RIGHT HAND	RT REACHING	0.28	-0.19	-0.14
	RT GRASPING	0.31	-0.15	-0.10
	MGA	**0.45**	0.08	0.17
LEFT HAND	RT REACHING	-0.05	0.19	-0.09
	RT GRASPING	-0.06	0.19	-0.09
	MGA	**0.37**	**0.45**	0.30

Run 1 after TMS: perturbed FC

		TRAINING DATASET		
		RIGHT-HAND DEXTERITY	RIGHT-HAND STRENGHT	LEFT-HAND STRENGHT
RIGHT HAND	RT REACHING	0.13	-0.29	-0.18
	RT GRASPING	0.18	-0.26	-0.14
	MGA	**0.46**	0.09	0.17
LEFT HAND	RT REACHING	-0.14	0.13	-0.24
	RT GRASPING	-0.13	0.10	-0.23
	MGA	**0.40**	**0.45**	**0.34**

Run 2 after TMS: perturbed FC

		TRAINING DATASET		
		RIGHT-HAND DEXTERITY	RIGHT-HAND STRENGHT	LEFT-HAND STRENGHT
RIGHT HAND	RT REACHING	0.09	-0.13	-0.12
	RT GRASPING	0.08	-0.07	-0.07
	MGA	0.08	0.17	0.13
LEFT HAND	RT REACHING	-0.01	0.08	-0.02
	RT GRASPING	0.00	0.06	-0.01
	MGA	0.24	0.08	0.23

p < 0.05 FDR corrected

Fig. 5. External validation results across rs-fMRI runs in an independent dataset. Prediction accuracy of CPM models trained on HCP data (columns) when applied to behavioral data from the independent dataset (rows). Behavioral variables include RT for grasping and reaching, and maximum grip aperture (MGA), for both hands. Red-highlighted cells mark significant predictions ($p < 0.05$, FDR corrected). A. Results from the first "unperturbed" rs-fMRI run acquired after sham TMS, but before real TMS stimulation. Significant predictions were observed for MGA of both hands, particularly when testing models trained on HCP dexterity and strength tasks. B. Results from the second "unperturbed" rs-fMRI run. The pattern largely replicates Panel A, with significant prediction for MGA of both hands, especially following training on dexterity and strength tasks for the corresponding hand. C. Results from the first rs-fMRI run after real TMS. Predictive performance remains comparable to pre-TMS runs, suggesting initial preservation of the network's functional architecture. D. Results from the second rs-fMRI run after real TMS. All prediction models failed to reach significance (all $p > 0.12$, uncorrected), suggesting a delayed effect of cTBS on the functional architecture of the core motor network.

strength for both hands), suggesting that the core CPM can capture general aspects of dexterous hand behavior, even across datasets.

Fig. 5B shows a similar pattern adopting the second "unperturbed" run of rs-fMRI (prior to real TMS). Significant predictions were again found for MGA of the right hand (training on right-hand dexterity) and for MGA of the left hand when training on either left-hand dexterity or strength ($p < 0.05$ FDR corrected). The prediction accuracy for MGA left-hand when training on strength left hand was close to the significant level (p uncorrected = 0.08) suggesting a trend toward generalizability in this condition.

To assess the potential impact of perturbation on the predictive power of the network, we tested the model on two additional "perturbed" rs-fMRI runs acquired after continuous theta-burst stimulation (cTBS) over the left inferior parietal cortex.

Fig. 5C shows the results from the rs-fMRI run acquired starting from approximately 5 min after real cTBS (the first post-TMS session). Despite the stimulation, prediction performance remained consistent with the pre-TMS state: MGA of the right hand was again significantly predicted from right-hand dexterity training, and MGA of the left hand was predicted from all three HCP models ($p < 0.05$ FDR corrected).

Fig. 5D shows the results from the final rs-fMRI run (the second post-TMS session) which was acquired later in time (approximately 15 min after TMS). Here, all model predictions failed to reach significance (all uncorrected p-values > 0.12). This suggests that cTBS affected the FC in the core network only at this time-point, suggesting that the effects of cTBS over the parietal area might take time to become evident. This is in line with a recent non-human primate investigation that demonstrated that the effects of cTBS on parietal cortex takes from 20 to 30 min to

reach its maximum effect (Romero et al., 2022).

All in all, these findings demonstrate that the core network CPM show generalization to novel motor-related variables from an independent dataset - i.e. MGA, a measure of fine hand motor control - and that its predictive performance is sensitive to TMS-induced modulation of parietal connectivity.

5. Discussion

The aim of this study was to investigate whether the encoding of general aspects of hand motor control is embedded in spontaneous FC. To this end, we adopted CPM on rs-FC to predict individual performance across a range of motor tasks.

Our first finding was the identification of a core hand motor network, derived from the intersection of significant connections across whole-brain CPMs for three motor tasks of the HCP dataset (right-hand dexterity, right- and left-hand strength). The core CPM predicted behavioral performance in these tasks, demonstrating that rs-FC contains information associated with distinctive features of the behavioural output.

Our second finding was the generalization of the prediction of the core CPM across different effectors and/or tasks. This seems to suggest that rs-FC in the core network captures also high-order aspects of hand functioning, not bound to specific motor outcomes.

Finally, we demonstrated that the core CPM generalized to an independent dataset featuring a different behavioural metric, i.e. MGA, further supporting the idea that the core network encodes task-independent information. Moreover, employing rs-FC acquired after TMS to hAIP, we could observe a time-dependent change in predictive power compatible with the effect of cTBS. This suggests that perturbed rs-FC affects the generalization of our core CPM.

In the next sections, we discuss the implications of our findings on the understanding of the nature of behavioral information embedded in spontaneous connectivity.

5.1. Distributed representation of task-specific motor information within spontaneous connectivity

We showed that distributed patterns of spontaneous connectivity in a widespread brain network could predict individual performance in specific motor tasks. In other words, our results reveal that hand action information is represented in a distributed way across the brain, even a rest. However, a limitation of this approach is that CPM focuses on describing the predictive role of connections within a network, rather than capturing the contribution of specific regions. As the core network was derived from the intersection of connections across three tasks, our interpretation of the specific role of these regions is indirect.

In addition, we acknowledge another limitation as the whole-brain and core models predicting left-hand dexterity were not significant. This weaker performance for left-hand dexterity may be attributable to the characteristics of our sample, which included only right-handed participants. Predictive power for dexterity was lower than for strength even in the dominant (right) hand, suggesting that dexterity may be inherently harder to model from rs-FC and/or that handedness plays a critical role. Future research should explore how hand dominance affects CPM performance, particularly for fine motor control tasks.

Despite these limitations, our findings are supported - and complementary to - recent fMRI studies (Livne et al., 2022; Zhang et al., 2023, 2025) which directly demonstrated the similarity between patterns of spontaneous brain activity and patterns of task-related activity associated with the performance of hand movements.

Livne et al. (2022) demonstrated that spontaneous activity in the primary motor cortex resembles task-evoked patterns of common, everyday hand actions more than uncommon ones, suggesting the motor cortex encodes frequently used movements even at rest. Extending this evidence, Zhang et al. (2023) demonstrated that spontaneous activity patterns in large-scale rs networks (Yeo et al., 2011) also exhibit different similarity with task-related patterns. The DAN aligned with patterns for common hand actions, while the VAN was more attuned to patterns for uncommon ones. This functional dissociation suggests that different rs networks may support distinct aspects of action representation even at rest. More recently, Zhang et al. (2025) showed that dynamic coactivation patterns linking the motor cortex with regions of large-scale rs networks (VAN, DAN, DMN) were preserved across rest and hand movements - even if they underwent a reconfiguration during the task. Taken together, these findings suggest that not only local spontaneous activity pattens (as in Livne et al., 2022; Zhang et al., 2023), but also distributed interactions between brain regions are critical for representing hand action at rest (Zhang et al., 2025), consistent with our data. Task-related information seems to be embedded within the intrinsic organization of these networks even in the absence of any explicit motor output, supporting the idea that these activity patterns code for behaviourally relevant information states.

Building on this evidence, it is tempting to interpret our findings within a framework proposing that resting-state activity and connectivity might be gradually shaped over the lifespan by everyday experience and learning mechanisms, thereby serving as functional scaffold or priors of task activation patterns (Petersen and Sporns, 2015; Raichle, 2011). Within this view, the specific type of information encoded within the connections of our core CPM is difficult to specify, as different aspects of our tasks might be represented (Gallivan and Culham, 2015). Task-specific predictions may encompass motor aspects of the actions, associated visual or somatosensory information or the sensory feedback generated by the movements. Future studies are therefore needed to disentangle the contributions of different rs-FC patterns to behaviorally relevant information and to clarify their role in supporting distinct components of hand motor control.

5.2. Representation of higher order aspects of hand motor control in spontaneous connectivity

We showed that the core CPM generalized its predictions across tasks, effectors and even datasets. This aspect of your findings is compelling, as it suggests rs-FC in the core network may encode information about hand behavior at a more abstract level, as indicated by our cross-generalization analyses (see Fig. 4). We can speculate about the type of higher-order information captured by our CPM comparing the commonalities between our strength and dexterity tasks. Both tasks require the specification of hand configurations to accomplish task demands. In the strength task, a specific posture of the hand must be maintained throughout the task, whereas in Nine-Hole Peg test, the hand is continuously reconfigured as pegs are inserted and removed. A plausible interpretation could be that the generalization of prediction of the CPM across these two tasks may imply that the core network encodes common neural principles underlying hand configuration shared across these different motor behaviors.

Our cross-generalization analyses support the idea that, like other cognitive domains, the motor system also relies on domain-general representations that are not exclusively tied to specific task requirements. This perspective aligns with recent evidence indicating that spontaneous activity can resemble task-evoked patterns associated with not only action execution (Zhang et al., 2023) but also action observation (Perciballi et al., 2025). These findings suggest that the core network might encode abstract, high-level regularities of action processing, rather than relying solely on task- or effector-specific features. Nonetheless, while these results demonstrated the presence of such representations within spontaneous connectivity, they do not fully clarify their precise informational content or functional role.

Additional insight comes from the external validation analysis (see Fig. 5), which showed that the core CPM generalized primarily to MGA, but not to RTs. This finding supports our proposal that CPM captures general aspects of motor control across tasks. RTs are influenced by task-

specific factors such as explicit instructions and attentional demands, whereas MGA reflects an implicit process largely independent of such factors. Indeed, MGA has been associated with visuo-motor transformations required to shape the fingers for performing hand-object interactions (Jeannerod et al., 1995; Rizzolatti et al., 1998; Rizzolatti and Luppino, 2001; Rizzolatti and Matelli, 2003). The representation of the required hand configuration is likely shared across all our motor tasks (strength, dexterity and grasping), a possibility further supported by the cTBS effect on CPM predictive power (see next section).

Following the interpretational framework proposed in the previous section (Petersen and Sporns, 2015; Raichle, 2011), we might view the coding of this task-independent information as embedded not only in task-specific activity but also in co-activation patterns of resting-state networks. In this sense, spontaneous connectivity may integrate not just task-specific features but also general aspects of motor control that are consistent across tasks.

A more speculative interpretation could be that these representations embedded in spontaneous activity might play a crucial role in prediction (Betti et al., 2021; Dimakou et al., 2025; Pezzulo et al., 2021). It has been proposed that the brain is actively maintaining and updating predictive representations relevant for future interactions with the environment even when “at rest” (Dimakou et al., 2025; Pezzulo et al., 2021). If so, spontaneous connectivity patterns might reflect latent functional architectures that support a more general anticipatory mechanism for predicting task-independent aspects of future actions even in the absence of overt movement.

5.3. *Specificity of modification of CPM’s predictive power following cTBS*

To the best of our knowledge, this is the first investigation to demonstrate that TMS can induce changes in the predictive power of a CPM. This finding suggests that informational states related to motor output, embedded in spontaneous activity, can be modified by external perturbation. Specifically, we observed a time-dependent decrease in the core model’s ability to predict MGA, consistent with the neurophysiological effects of cTBS on parietal cortex, which unfold gradually to reach their maximum (Romero et al., 2022). We acknowledge that we cannot fully exclude that the described effect might be driven by unspecific factors – such as change in arousal across the experimental session or time-dependent drifts in rs-fMRI signal. Still, the specificity of this effect seems to support the idea that spontaneous connectivity carries representational content closely related to task-evoked activity.

The stimulated region, hAIP, is known to be an important node involved in the visuo-motor transformation for producing hand motor commands (Jeannerod et al., 1995; Rizzolatti et al., 1998; Rizzolatti and Luppino, 2001; Rizzolatti and Matelli, 2003). Previous studies have shown that TMS over hAIP impairs performance during hand actions (Breveglieri et al., 2023; Glover et al., 2005; Gutteling et al., 2013; Rice et al., 2007, 2006; Tunik et al., 2008, 2005). More recently, a lesion study identified hAIP as causally involved in modifications of hand preshaping, as measured by MGA, during visually guided grasping (Di Caro et al., 2025). This corpus of evidence supports a functional relationship - and possibly an equivalence - between information encoded within the hAIP during hand motor tasks and during rest. By directly demonstrating that transient perturbations of rs-FC can alter CPM predictions, our study supports the functional relevance of spontaneous connectivity patterns, supporting prior reports linking rs modifications to learning (Guerra-Carrillo et al., 2014) and to neurological disorders (Hohenfeld et al., 2018).

5.4. *Methodological considerations on our analytical approach*

While our findings provide evidence for a "core network" involved in hand actions, several methodological limitations warrant consideration. First, the use of the CPM framework focuses on the predictive role of network-wide connections rather than the specific anatomical contribution of individual regions. Moreover, this network was identified through a data-driven approach, as the intersection of connections across three distinct tasks. Consequently, any interpretation of the specific functional role of each brain region is inherently indirect.

Second, although the observed cTBS effects on the parietal cortex are consistent with our previous study (Pierotti et al., 2025) and align with effect identified in non-human primate studies (Romero et al., 2022), we cannot completely exclude non-specific factors affecting our neurostimulation-related findings. Potential confounds—such as time-dependent signal drift in the resting-state fMRI data or fluctuations in participant arousal over the duration of the experimental session—may have influenced the results. Future studies employing active control stimulation sites or tighter behavioral controls for arousal could further isolate the specific neuromodulatory impact of cTBS on this core network.

6. Conclusions

We identified a core hand motor network whose rs-FC predicts individual behavioral performance across distinct motor tasks and generalizes its prediction across effectors, tasks and datasets. Our data converge with growing evidence that spontaneous brain activity has a representational role, embedding behaviorally-relevant information that ranges from local motor features to higher-order task-independent principles of action control. By showing that these representations are distributed, generalizable and sensitive to external perturbation, we provide novel insights into the functional relevance of resting-state connectivity. Our description provides the starting point for investigating how alterations in spontaneous connectivity may also characterise motor impairments in neurological conditions.

Declaration of generative AI and AI-assisted technologies in the writing process

During the preparation of this work the authors adopted AI only to improve the clarity and readability of the manuscript text.

Research data sharing statement

The data that support the findings of this study are available on reasonable request from the corresponding author. The use of the data should be in line with the purpose of informed consent signed by the participants.

CRediT authorship contribution statement

Enrica Pierotti: Writing – review & editing, Writing – original draft, Visualization, Software, Investigation, Formal analysis, Data curation. **Luigi Cattaneo:** Writing – review & editing, Investigation, Conceptualization. **Luca Turella:** Writing – review & editing, Writing – original draft, Visualization, Supervision, Software, Project administration, Funding acquisition, Formal analysis, Conceptualization.

Declaration of competing interest

The authors declare that they have no known competing financial interests or personal relationships that could have appeared to influence the work reported in this paper.

Acknowledgements

This work was supported by the European Union – Next Generation EU, in the framework of the project MNESYS - A MULTISCALE INTEGRATED APPROACH TO THE STUDY OF THE NERVOUS SYSTEM IN HEALTH AND DISEASE (Prot. n. PE00000006). This work was also supported by the European Union - Next Generation EU PRIN 2022 (DD

104 02/02/22) – PNRR – M4 – C2 – INV1.1 – PRIN –Project Title [COMPArative charACTterization of the parietal lobe: a multimodal approach (COMPAACT project)] – project identifier code [2022JT852C] – CUP [E53D23022180006]. The views and opinions expressed are solely those of the authors and do not necessarily reflect those of the European Union, nor can the European Union be held responsible for them.

Data for the CPM definition were provided by the Human Connectome Project, WU-Minn Consortium (Principal Investigators: David Van Essen and Kamil Ugurbil; 1U54MH091657) funded by the 16 NIH Institutes and Centers that support the NIH Blueprint for Neuroscience Research; and by the McDonnell Center for Systems Neuroscience at Washington University.

Supplementary materials

Supplementary material associated with this article can be found, in the online version, at doi:10.1016/j.neuroimage.2026.121883.

References

Avery, E.W., Yoo, K., Rosenberg, M.D., Greene, A.S., Gao, S., Na, D.L., Scheinost, D., Constable, T.R., Chun, M.M., 2020. Distributed patterns of functional connectivity predict working memory performance in novel healthy and memory-impaired individuals. J. Cogn. Neurosci. 32, 241–255. https://doi.org/10.1162/jocn_a_01487.

Beaty, R.E., Kenett, Y.N., Christensen, A.P., Rosenberg, M.D., Benedek, M., Chen, Q., Fink, A., Qiu, J., Kwapil, T.R., Kane, M.J., Silvia, P.J., 2018. Robust prediction of individual creative ability from brain functional connectivity. Proc. Natl. Acad. Sci. U.S.A. 115, 1087–1092. https://doi.org/10.1073/pnas.1713532115.

Benjamini, Y., Hochberg, Y., 1995. Controlling the false discovery rate: a practical and powerful approach to multiple. Source: J. R. Stat. Soc. B (Methodol.) 57, 289–300.

Betti, V., Della Penna, S., De Pasquale, F., Corbetta, M., 2021. Spontaneous beta band rhythms in the predictive coding of natural stimuli. Neuroscientist 27, 184–201. https://doi.org/10.1177/1073858420928988.

Biswal, B.B., Uddin, L.Q., 2025. The history and future of resting-state functional magnetic resonance imaging. Nature 641, 1121–1131. https://doi.org/10.1038/s41586-025-08953-9.

Breveglieri, R., Borgomaneri, S., Filippini, M., Tessari, A., Galletti, C., Davare, M., Fattori, P., 2023. Complementary contribution of the medial and lateral human parietal cortex to grasping: a repetitive TMS study. Cereb. Cortex 33, 5122–5134. https://doi.org/10.1093/cercor/bhac404.

Budisavljevic, S., Dell'Acqua, F., Zanatto, D., Begliomini, C., Miotto, D., Motta, R., Castiello, U., 2017. Asymmetry and Structure of the Fronto-Parietal Networks Underlie Visuomotor Processing in Humans. Cereb. Cortex 27, 1532–1544. https://doi.org/10.1093/cercor/bhv348.

Cai, H., Chen, J., Liu, S., Zhu, J., Yu, Y., 2020. Brain functional connectome-based prediction of individual decision impulsivity. Cortex 125, 288–298. https://doi.org/10.1016/j.cortex.2020.01.022.

Culham, J.C., Cavina-Pratesi, C., Singhal, A., 2006. The role of parietal cortex in visuomotor control: what have we learned from neuroimaging? Neuropsychologia 44, 2668–2684. https://doi.org/10.1016/j.neuropsychologia.2005.11.003.

Culham, J.C., Valyear, K.F., 2006. Human parietal cortex in action. Curr. Opin. Neurobiol. 16, 205–212. https://doi.org/10.1016/j.conb.2006.03.005.

Di Caro, V., Cesari, P., Sala, F., Cattaneo, L., 2025. The neural bases of the reach–grasp movement in humans: quantitative evidence from brain lesions. Proc. Natl. Acad. Sci. U.S.A. 122. https://doi.org/10.1073/pnas.2419801122.

Dimakou, A., Pezzulo, G., Zangrossi, A., Corbetta, M., 2025. The predictive nature of spontaneous brain activity across scales and species. Neuron 1–23. https://doi.org/10.1016/j.neuron.2025.02.009.

Errante, A., Ziccarelli, S., Mingolla, G., Fogassi, L., 2021. Grasping and manipulation: neural bases and anatomical circuitry in humans. Neuroscience 458, 203–212. https://doi.org/10.1016/j.neuroscience.2021.01.028.

Finn, E.S., Shen, X., Scheinost, D., Rosenberg, M.D., Huang, J., Chun, M.M., Papademetris, X., Constable, R.T., 2015. Functional connectome fingerprinting: identifying individuals using patterns of brain connectivity. Nat. Neurosci. 18, 1664–1671. https://doi.org/10.1038/nn.4135.

Gallivan, J.P., Culham, J.C., 2015. Neural coding within human brain areas involved in actions. Curr. Opin. Neurobiol. 33, 141–149. https://doi.org/10.1016/j.conb.2015.03.012.

Gallivan, J.P., McLean, D.A., Flanagan, J.R., Culham, J.C., 2013. Where one hand meets the other: limb-specific and action-dependent movement plans decoded from preparatory signals in single human frontoparietal brain areas. J. Neurosci. 33, 1991–2008. https://doi.org/10.1523/JNEUROSCI.0541-12.2013.

Gallivan, J.P., McLean, D.A., Valyear, K.F., Pettypiece, C.E., Culham, J.C., 2011. Decoding action intentions from preparatory brain activity in human parieto-frontal networks. J. Neurosci. 31, 9599–9610. https://doi.org/10.1523/JNEUROSCI.0080-11.2011.

Glasser, M.F., Coalson, T.S., Robinson, E.C., Hacker, C.D., Harwell, J., Yacoub, E., Ugurbil, K., Andersson, J., Beckmann, C.F., Jenkinson, M., Smith, S.M., Van Essen, D. C., 2016. A multi-modal parcellation of human cerebral cortex. Nature 536, 171–178. https://doi.org/10.1038/nature18933.

Glasser, M.F., Sotiropoulos, S.N., Wilson, J.A., Coalson, T.S., Fischl, B., Andersson, J.L., Xu, J., Jbabdi, S., Webster, M., Polimeni, J.R., Van Essen, D.C., Jenkinson, M., 2013. The minimal preprocessing pipelines for the Human Connectome Project. NeuroImage 80, 105–124. https://doi.org/10.1016/j.neuroimage.2013.04.127.

Glover, S., Miall, R.C., Rushworth, M.F.S., 2005. Parietal rTMS disrupts the initiation but not the execution of on-line adjustments to a perturbation of object size. J. Cogn. Neurosci. 17, 124–136. https://doi.org/10.1162/0898929052880066.

Gordon, E.M., Laumann, T.O., Adeyemo, B., Huckins, J.F., Kelley, W.M., Petersen, S.E., 2016. Generation and evaluation of a cortical area parcellation from resting-State correlations. Cereb. Cortex 26, 288–303. https://doi.org/10.1093/cercor/bhu239.

Grafton, S.T., 2010. The cognitive neuroscience of prehension: recent developments. Exp. Brain Res. 204, 475–491. https://doi.org/10.1007/s00221-010-2315-2.

Grefkes, C., Fink, G.R., 2005. The functional organization of the intraparietal sulcus in humans and monkeys. J. Anat. 207, 3–17. https://doi.org/10.1111/j.1469-7580.2005.00426.x.

Griffanti, L., Salimi-Khorshidi, G., Beckmann, C.F., Auerbach, E.J., Douaud, G., Sexton, C. E., Zsoldos, E., Ebmeier, K.P., Filippini, N., Mackay, C.E., Moeller, S., Xu, J., Yacoub, E., Baselli, G., Ugurbil, K., Miller, K.L., Smith, S.M., 2014. ICA-based artefact removal and accelerated fMRI acquisition for improved resting state network imaging. NeuroImage 95, 232–247. https://doi.org/10.1016/j.neuroimage.2014.03.034.

Guerra-Carrillo, B., Mackey, A.P., Bunge, S.A., 2014. Resting-State fMRI: a window into Human brain plasticity. Neuroscientist 20, 522–533. https://doi.org/10.1177/1073858414524442.

Gutteling, T.P., Park, S.Y., Kenemans, J.L., Neggers, S.F.W., 2013. TMS of the anterior intraparietal area selectively modulates orientation change detection during action preparation. J. Neurophysiol. 110, 33–41. https://doi.org/10.1152/jn.00622.2012.

Haufe, S., Meinecke, F., Görgen, K., Dähne, S., Haynes, J.D., Blankertz, B., Bießmann, F., 2014. On the interpretation of weight vectors of linear models in multivariate neuroimaging. NeuroImage 87, 96–110. https://doi.org/10.1016/j.neuroimage.2013.10.067.

Hodes, R.J., Insel, T.R., Landis, S.C., 2013. The NIH Toolbox. Neurology 80, 2013. https://doi.org/10.1212/WNL.0b013e3182872e90.

Hohenfeld, C., Werner, C.J., Reetz, K., 2018. Resting-state connectivity in neurodegenerative disorders: is there potential for an imaging biomarker? NeuroImage: Clin. 18, 849–870. https://doi.org/10.1016/j.nicl.2018.03.013.

Hsu, W.-T., Rosenberg, M.D., Scheinost, D., Constable, R.T., Chun, M.M., 2018. Resting-state functional connectivity predicts neuroticism and extraversion in novel individuals. Soc. Cogn. Affect. Neurosci. 13, 224–232. https://doi.org/10.1093/scan/nsy002.

Huang, Y.Z., Edwards, M.J., Rounis, E., Bhatia, K.P., Rothwell, J.C., 2005. Theta burst stimulation of the human motor cortex. Neuron 45, 201–206. https://doi.org/10.1016/j.neuron.2004.12.033.

Jeannerod, M., Arbib, M.A., Rizzolatti, G., Sakata, H., 1995. Grasping objects: the cortical mechanisms of visuomotor transformation. Trends Neurosci. 18, 314–320. https://doi.org/10.1016/0166-2236(95)93921-J.

Jiang, R., Calhoun, V.D., Zuo, N., Lin, D., Li, J., Fan, L., Qi, S., Sun, H., Fu, Z., Song, M., Jiang, T., Sui, J., 2018. Connectome-based individualized prediction of temperament trait scores. NeuroImage 183, 366–374. https://doi.org/10.1016/j.neuroimage.2018.08.038.

Kim, J., Andrews-Hanna, J.R., Eisenbarth, H., Lux, B.K., Kim, H.J., Lee, E., Lindquist, M. A., Losin, E.A.R., Wager, T.D., Woo, C.W., 2023. A dorsomedial prefrontal cortex-based dynamic functional connectivity model of rumination. Nat. Commun. 14, 1–14. https://doi.org/10.1038/s41467-023-39142-9.

Lake, E.M.R., Finn, E.S., Noble, S.M., Vanderwal, T., Shen, X., Rosenberg, M.D., Spann, M.N., Chun, M.M., Scheinost, D., Constable, R.T., 2019. The functional brain organization of an individual allows prediction of measures of social abilities transdiagnostically in autism and Attention-Deficit/Hyperactivity Disorder. Biol. Psychiatry 86, 315–326. https://doi.org/10.1016/j.biopsych.2019.02.019.

Livne, T., Kim, D., Metcalf, N.V., Zhang, L., Pini, L., Shulman, G.L., Corbetta, M., 2022. Spontaneous activity patterns in human motor cortex replay evoked activity patterns for hand movements. Sci. Rep. 12. https://doi.org/10.1038/s41598-022-20866-5.

Malfatti, G., Turella, L., 2021. Neural encoding and functional interactions underlying pantomimed movements. Brain Struct. Funct. 226, 2321–2337. https://doi.org/10.1007/s00429-021-02332-6.

Mathiowetz, V., Weber, K., Kashman, N., Volland, G., 1985. Adult norms for the nine hole peg test of finger dexterity. Occup. Ther. J. Res. 5, 24–38. https://doi.org/10.1177/153944928500500102.

Monaco, S., Malfatti, G., Culham, J.C., Cattaneo, L., Turella, L., 2020. Decoding motor imagery and action planning in the early visual cortex: overlapping but distinct neural mechanisms. NeuroImage 218, 116981. https://doi.org/10.1016/j.neuroimage.2020.116981.

Monaco, S., Malfatti, G., Zendron, A., Pellencin, E., Turella, L., 2019. Predictive coding of action intentions in dorsal and ventral visual stream is based on visual anticipations, memory-based information and motor preparation. Brain Struct. Funct. 224, 3291–3308. https://doi.org/10.1007/s00429-019-01970-1.

Nettekoven, C., Zhi, D., Shahshahani, L., Pinho, A.L., Saadon-grosman, N., Diedrichsen, J., 2023. A hierarchical atlas of the human cerebellum for functional precision mapping. bioRxiv 1–27. https://doi.org/10.1101/2023.09.14.557689.

Oldfield, R.C., 1971. The assessment and analysis of handedness: the Edinburgh inventory. Neuropsychologia 9, 97–113. https://doi.org/10.1016/0028-3932(71)90067-4.

Perciballi, C., Pini, L., Sili, D., Rassi, Y.E., Zhang, L., Handjaras, G., Giove, F., Ricciardi, E., Corbetta, M., Betti, V., 2025. How spontaneous brain activity encodes

the observation of grasping movements. NeuroImage 318, 121396. https://doi.org/10.1016/j.neuroimage.2025.121396.
Petersen, S.E., Sporns, O., 2015. Brain networks and cognitive architectures. Neuron 88, 207–219. https://doi.org/10.1016/j.neuron.2015.09.027.
Pezzulo, G., Zorzi, M., Corbetta, M., 2021. The secret life of predictive brains: what's spontaneous activity for? Trends Cogn. Sci. (Regul. Ed.) 25, 730–743. https://doi.org/10.1016/j.tics.2021.05.007.
Pierotti, E., Speranza, C., Cattaneo, L., Turella, L., 2025. Investigating resting-state functional connectivity of the human hand motor system: an offline TMS-fMRI study. NeuroImage 314, 121254. https://doi.org/10.1016/j.neuroimage.2025.121254.
Rabini, G., Pierotti, E., Meli, C., Dodich, A., Papagno, C., Turella, L., 2023. Connectome-based fingerprint of motor impairment is stable along the course of Parkinson's disease. Cereb. Cortex 33, 9896–9907. https://doi.org/10.1093/cercor/bhad252.
Raichle, M.E., 2011. The Restless Brain. Brain Connect. 1, 3–12. https://doi.org/10.1089/brain.2011.0019.
Rice, N.J., Tunik, E., Cross, E.S., Grafton, S.T., 2007. On-line grasp control is mediated by the contralateral hemisphere. Brain Res. 1175, 76–84. https://doi.org/10.1016/j.brainres.2007.08.009.
Rice, N.J., Tunik, E., Grafton, S.T., 2006. The anterior intraparietal sulcus mediates grasp execution, independent of requirement to update: new insights from transcranial magnetic stimulation. J. Neurosci. 26, 8176–8182. https://doi.org/10.1523/JNEUROSCI.1641-06.2006.
Rizzolatti, G., Luppino, G., 2001. The cortical motor system. Neuron 31, 889–901.
Rizzolatti, G., Luppino, G., Matelli, M., 1998. The organization of the cortical motor system: new concepts. Electroencephalogr. Clin. Neurophysiol. 106, 283–296. https://doi.org/10.3892/ijmm.16.5.911.
Rizzolatti, G., Matelli, M., 2003. Two different streams form the dorsal visual system: anatomy and functions. Exp. Brain Res. 153, 146–157. https://doi.org/10.1007/s00221-003-1588-0.
Romero, M.C., Merken, L., Janssen, P., Davare, M., 2022. Neural effects of continuous theta-burst stimulation in macaque parietal neurons. eLife 11, 1–19. https://doi.org/10.7554/eLife.65536.
Rosenberg, M.D., Finn, E.S., Scheinost, D., Constable, R.T., Chun, M.M., 2017. Characterizing Attention with Predictive Network Models. Tre. in Cogn. Sci 21, 290–302. https://doi.org/10.1016/j.tics.2017.01.011.
Rosenberg, M.D., Hsu, W.-T., Scheinost, D., Todd Constable, R., Chun, M.M., 2018. Connectome-based models predict separable components of attention in novel individuals. J. Cogn. Neurosci. 30, 160–173. https://doi.org/10.1162/jocn_a_01197.
Rosenberg, M.D., Scheinost, D., Greene, A.S., Avery, E.W., Kwon, Y.H., Finn, E.S., Ramani, R., Qiu, M., Constable, R.T., Chun, M.M., 2020. Functional connectivity predicts changes in attention observed across minutes, days, and months. Proc. Natl. Acad. Sci. U.S.A. 117, 3797–3807. https://doi.org/10.1073/pnas.1912226117.
Rosenberg, M.D., Zhang, S., Hsu, W.T., Scheinost, D., Finn, E.S., Shen, X., Constable, R.T., Li, C.S.R., Chun, M.M., 2016. Methylphenidate modulates functional network connectivity to enhance attention. J. Neurosci. 36, 9547–9557. https://doi.org/10.1523/JNEUROSCI.1746-16.2016.
Ruck, L., Schoenemann, P.T., 2021. Handedness measures for the Human Connectome Project: implications for data analysis. Laterality 26, 584–606. https://doi.org/10.1080/1357650X.2020.1866001.
Salimi-Khorshidi, G., Douaud, G., Beckmann, C.F., Glasser, M.F., Griffanti, L., Smith, S. M., 2014. Automatic denoising of functional MRI data: combining independent component analysis and hierarchical fusion of classifiers. NeuroImage 90, 449–468. https://doi.org/10.1016/j.neuroimage.2013.11.046.
Sartin, S., Ranzini, M., Scarpazza, C., Monaco, S., 2023. Cortical areas involved in grasping and reaching actions with and without visual information: an ALE meta-analysis of neuroimaging studies. Curr. Res. Neurobiol. 4, 100070. https://doi.org/10.1016/j.crneur.2022.100070.
Schaefer, A., Kong, R., Gordon, E.M., Laumann, T.O., Zuo, X.-N., Holmes, A.J., Eickhoff, S.B., Yeo, B.T.T., 2018. Local-global parcellation of the Human cerebral cortex from intrinsic functional connectivity MRI. Cereb. Cortex 28, 3095–3114. https://doi.org/10.1093/cercor/bhx179.
Scheinost, D., Noble, S., Horien, C., Greene, A.S., Lake, E.M., Salehi, M., Gao, S., Shen, X., O'Connor, D., Barron, D.S., Yip, S.W., Rosenberg, M.D., Constable, R.T., 2019. Ten simple rules for predictive modeling of individual differences in neuroimaging. NeuroImage 193, 35–45. https://doi.org/10.1016/j.neuroimage.2019.02.057.
Shen, X., Finn, E.S., Scheinost, D., Rosenberg, M.D., Chun, M.M., Papademetris, X., Constable, R.T., 2017. Using connectome-based predictive modeling to predict individual behavior from brain connectivity. Nat. Protoc. 12, 506–518. https://doi.org/10.1038/nprot.2016.178.
Smith, S.M., Beckmann, C.F., Andersson, J., Auerbach, E.J., Bijsterbosch, J., Douaud, G., Duff, E., Feinberg, D.A., Griffanti, L., Harms, M.P., Kelly, M., Laumann, T., Miller, K. L., Moeller, S., Petersen, S., Power, J., Salimi-Khorshidi, G., Snyder, A.Z., Vu, A.T., Woolrich, M.W., Xu, J., Yacoub, E., Uğurbil, K., Van Essen, D.C., Glasser, M.F., 2013. Resting-state fMRI in the human connectome project. NeuroImage 80, 144–168. https://doi.org/10.1016/j.neuroimage.2013.05.039.
Thomas Yeo, B.T., Krienen, F.M., Sepulcre, J., Sabuncu, M.R., Lashkari, D., Hollinshead, M., Roffman, J.L., Smoller, J.W., Zöllei, L., Polimeni, J.R., Fischl, B., Liu, H., Buckner, R.L., 2011. The organization of the human cerebral cortex estimated by intrinsic functional connectivity. J. Neurophysiol. 106, 1125–1165. https://doi.org/10.1152/jn.00338.2011.
Tunik, E., Frey, S.H., Grafton, S.T., 2005. Virtual lesions of the anterior intraparietal area disrupt goal-dependent on-line adjustments of grasp. Nat. Neurosci. 8, 505–511. https://doi.org/10.1038/nn1430.
Tunik, E., Lo, O.Y., Adamovich, S.V., 2008. Transcranial magnetic stimulation to the frontal operculum and supramarginal gyrus disrupts planning of outcome-based hand-object interactions. J. Neurosci. 28, 14422–14427. https://doi.org/10.1523/JNEUROSCI.4734-08.2008.
Turella, L., Lingnau, A., 2014. Neural correlates of grasping. Front. Hum. Neurosci. 8, 1–8. https://doi.org/10.3389/fnhum.2014.00686.
Turella, L., Rumiati, R., Lingnau, A., 2020. Hierarchical action encoding within the Human brain. Cereb. Cortex 30, 2924–2938. https://doi.org/10.1093/cercor/bhz284.
Van Essen, D.C., Smith, S.M., Barch, D.M., Behrens, T.E.J., Yacoub, E., Ugurbil, K., 2013. The WU-Minn human connectome project: an overview. NeuroImage 80, 62–79. https://doi.org/10.1016/j.neuroimage.2013.05.041.
Van Essen, D.C., Ugurbil, K., Auerbach, E., Barch, D., Behrens, T.E.J., Bucholz, R., Chang, A., Chen, L., Corbetta, M., Curtiss, S.W., Della Penna, S., Feinberg, D., Glasser, M.F., Harel, N., Heath, A.C., Larson-Prior, L., Marcus, D., Michalareas, G., Moeller, S., Oostenveld, R., Petersen, S.E., Prior, F., Schlaggar, B.L., Smith, S.M., Snyder, A.Z., Xu, J., Yacoub, E., 2012. The human connectome project: a data acquisition perspective. NeuroImage 62, 2222–2231. https://doi.org/10.1016/j.neuroimage.2012.02.018.
Vesia, M., Crawford, J.D., 2012. Specialization of reach function in human posterior parietal cortex. Exp. Brain Res. 221, 1–18. https://doi.org/10.1007/s00221-012-3158-9.
Wu, J., Eickhoff, S.B., Hoffstaedter, F., Patil, K.R., Schwender, H., Thomas Yeo, B.T., Genon, S., 2021. A connectivity-based psychometric prediction framework for brain-behavior relationship studies. Cereb. Cortex 31, 3732–3751. https://doi.org/10.1093/cercor/bhab044.
Wu, J., Li, J., Eickhoff, S.B., Hoffstaedter, F., Hanke, M., Yeo, B.T.T., Genon, S., 2022. Cross-cohort replicability and generalizability of connectivity-based psychometric prediction patterns. NeuroImage 262, 119569. https://doi.org/10.1016/j.neuroimage.2022.119569.
Wu, J., Li, J., Eickhoff, S.B., Scheinost, D., Genon, S., 2023. The challenges and prospects of brain-based prediction of behaviour. Nat. Hum. Behav. 7, 1255–1264. https://doi.org/10.1038/s41562-023-01670-1.
Yeo, B.T., Krienen, F.M., Sepulcre, J., Sabuncu, M.R., Lashkari, D., Hollinshead, M., Roffman, J.L., Smoller, J.W., Zöllei, L., Polimeni, J.R., Fischl, B., Liu, H., Buckner, R. L., 2011. The organization of the human cerebral cortex estimated by intrinsic functional connectivity. J. Neuro. 106, 1125–1165. https://doi.org/10.1152/jn.00338.2011.
Yoo, K., Rosenberg, M.D., Hsu, W.-T., Zhang, S., Li, C.-S.R., Scheinost, D., Constable, R. T., Chun, M.M., 2018. Connectome-based predictive modeling of attention: comparing different functional connectivity features and prediction methods across datasets. NeuroImage 167, 11–22. https://doi.org/10.1016/j.neuroimage.2017.11.010.
Yoo, K., Rosenberg, M.D., Kwon, Y.H., Lin, Q., Avery, E.W., Sheinost, D., Constable, R.T., Chun, M.M., 2022. A brain-based general measure of attention. Nat. Hum. Behav. 6, 782–795. https://doi.org/10.1038/s41562-022-01301-1.
Yoo, K., Rosenberg, M.D., Noble, S., Scheinost, D., Constable, R.T., Chun, M.M., 2019. Multivariate approaches improve the reliability and validity of functional connectivity and prediction of individual behaviors. NeuroImage 197, 212–223. https://doi.org/10.1016/j.neuroimage.2019.04.060.
Zhang, H., Hao, S., Lee, A., Eickhoff, S.B., Pecheva, D., Cai, S., Meaney, M., Chong, Y., Broekman, B.F.P., Fortier, M.V., Qiu, A., 2020. Do intrinsic brain functional networks predict working memory from childhood to adulthood? Hum. Brain Mapp. 41, 4574–4586. https://doi.org/10.1002/hbm.25143.
Zhang, L., Pini, L., Kim, D., Shulman, G.L., Corbetta, M., 2023. Spontaneous activity patterns in Human attention networks code for hand movements. J. Neurosci. 43, 1976–1986. https://doi.org/10.1523/jneurosci.1601-22.2023.
Zhang, L., Pini, L., Shulman, G.L., Corbetta, M., 2025. Brain-wide dynamic coactivation states code for hand movements in the resting state. Proc. Natl. Acad. Sci. 122, 2017. https://doi.org/10.1073/pnas.2415508122.